Modelling and experimental verification of a solar reactor for photo-Fenton treatment

J. Farias, E. D. Albizzati and O. M. Alfano

ABSTRACT

In the present work, a novel design of a solar reactor is presented. This pilot plant scale reactor uses the UV-Visible and Near-Infrared solar radiation to promote the photo-Fenton treatment. A theoretical study and experimental verification were performed using formic acid as a model pollutant. The radiative transfer, thermal energy and mass balances equations were solved to compute the formic acid (F) and hydrogen peroxide (P) concentrations as a function of time. The spectral and broadband solar radiation incident on the reactor window was calculated from a computational code: the SMARTS2 program. Statistical estimators have been used to measure the departure of theoretical model from experimental data. A good agreement for formic acid and hydrogen peroxide concentrations, temperature and total and UV broadband solar radiation was obtained. The normalized root mean square errors (NRMSE) of the model for predicted variables were lower than 11%.

Key words | photo-Fenton treatment, pilot plant scale reactor, solar reactor, UV solar radiation

J. Farias
O. M. Alfano (corresponding author)
INTEC (Universidad Nacional del Litoral and CONICET),
Ruta No. 168,
3000 Santa Fe,
Argentina
E-mail: *alfano@conicet-santafe.gob.ar*

E. D. Albizzati
Facultad de Ingeniería Química,
UNL,
S. del Estero,
2654 Santa Fe,
Argentina

INTRODUCTION

The feasibility of applying solar radiation has made the photo-Fenton system an economical and competitive process. It has been demonstrated that the Fenton degradation of pollutants can be considerably improved by UV/visible radiation and the temperature increase. Sagawe *et al.* (2001) have employed a model pollutant, the 4-nitrophenol, to study the influence of operating parameters such as temperature and reactor depth on the Fenton and photo-Fenton processes. Then, Gernjak *et al.* (2006) have investigated the degradation of alachlor in a compound parabolic collector (CPC) solar reactor, to evaluate the effects of temperature, iron concentration and illuminated volume on the pollutant degradation. Farias *et al.* (2007) have studied the effects of the reaction temperature and the solar radiation on the Fenton degradation rate of the formic acid; they found that when the temperature is low (25°C), the pollutant conversion enhancement is significantly increased by irradiation, and when the temperature is relatively high (55°C), this effect is less important (a pollutant conversion enhancement of 7.4%). Recently, Zapata *et al.* (2009) have evaluated the degradation of a commercial pesticide mixture in a pilot-plant photo-Fenton reactor at the Plataforma Solar de Almería; they found that the process efficiency gradually increases with the reaction temperature, but at 50°C this efficiency decreases. Finally, Monteagudo *et al.* (2009), have performed an experimental study with the non-biodegradable azo dye Orange II in a solar CPC and evaluated the influence of continuous addition of hydrogen peroxide and air injection on the decoloration rate and TOC removal. An interesting and complete review on the use of sunlight to generate hydroxyl radicals by titanium dioxide photocatalysis and photo-Fenton process, for decontamination and disinfection of water, was published by Malato *et al.* (2009).

It is known that the performance of solar technologies presents a strong dependence on the incident energy. So, fluctuations of the solar irradiance with time should be

doi: 10.2166/wst.2010.047

considered in the degradation of pollutants (Alfano *et al.* 2000). In the present work, a novel design of a solar reactor is presented. This pilot-plant photoreactor is a hybrid solar unit that captures the thermal and photochemical solar radiation. A theoretical study and experimental verification were performed using formic acid as a model pollutant. It was possible evaluating the photo-Fenton reaction rate for each reaction time. To do this, we have solved the thermal energy and mass balances and the radiative transfer Equation (RTE) together with spectral UV–total broadband solar radiation.

EXPERIMENTAL SOLAR REACTOR

A flat-plate solar reactor has been built for photo-Fenton treatment because of the benefit effect of solar energy in the degradation rate of pollutants. Figure 1(a) shows a flow sheet of the experimental device and Figure 1(b) gives details of the solar reactor. The experimental system is comprised by a reactor, a storage tank, tubing and a circulation pump. The reactor entry aperture is tilted towards the north according to the latitude.

The newly designed non-concentrating photoreactor is a thermally insulated box with a black solar energy-absorbing surface and a two-plate UV-transparent window. This system transforms the solar radiation to heat and captures the UV solar radiation. The fluid in the reactor circulates through two channels. When the solution flows through the upper channel is heated and absorbs UV radiation (photo-Fenton reaction). In the lower channel it is pre-heated.

Experiments

The solutions of formic acid (Merck, ACS), hydrogen peroxide (Carlo Erba, ACS, 30%) and ferric sulphate (Carlo Erba, RPE) were prepared with distilled water. The experimental run began when a ferric sulphate solution was added to formic acid solution into the tank and the pH was adjusted to 3. During the initial period of each experimental run, the reactor window was covered with an opaque plate to avoid solar irradiation entrance. Then, the hydrogen peroxide solution was added to the tank, the valve was opened to allow a solution flow rate of $4\,\mathrm{L\,min^{-1}}$ into reactor and the first sample was withdrawn. Finally, the shutter was removed; this operation determined the starting time of the photo-Fenton reaction. As soon as the sample was withdrawn, the reaction was stopped suddenly by adding sodium sulphite. Formic acid was analyzed with total organic carbon measurement (Shimadzu TOC–5000A). For the measurement of hydrogen peroxide, a modified iodometric technique was used (Allen *et al.* 1952). Ferrous ions were tested with absorbance measurements of the Fe(II)-phenantroline complex at a wavelength of 510 nm (APHA 1995). Table 1 shows the operating conditions for the experiments, where C_F^0 is the initial formic acid concentration and X_F the formic acid conversion. The modified variables are: ferric initial

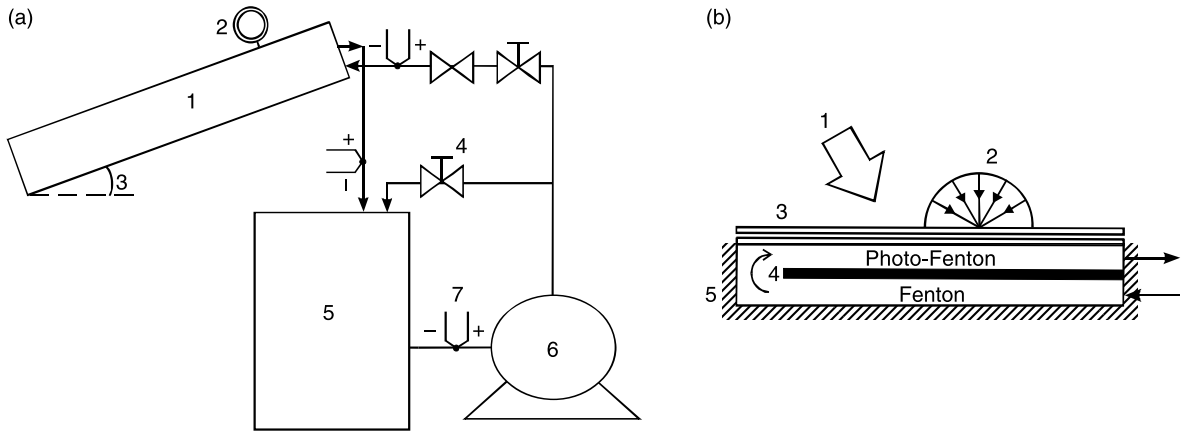

Figure 1 | (a) Experimental device: (1) solar reactor, (2) radiometer, (3) tilt, (4) valve, (5) tank, (6) pump, (7) thermocouple. (b) Solar reactor: (1) direct radiation, (2) diffuse radiation, (3) window, (4) absorbent plate, (5) thermal insulation.

Table 1 | Operating conditions and formic acid conversions ($C_F^0 = 3$ mM)

N	Reaction	Fe(III) (ppm)	R	T_0 (°C)	Start time (h)	Duration (h)	$X_{F,210\,min}$ (%)
1	Photo-Fenton	1.8	1.5	25	10.5	3.5	75.0
2	Photo-Fenton	0.8	1.8	44*	12.5	3.5	85.0
3	Photo-Fenton	3.4	2.2	32	12.5	3.5	98.0
4	Photo-Fenton	0.8	1.8	31	13.0	4.5	70.7†
5	Fenton	3.2	1.9	31	12.5	4.5	54.0†
6	Photo-Fenton	0.8	3.1	27	10.8	4.5	80.5†

*Pre-heated solution.
†Pollutant conversion after 225 min.

concentrations (Fe(III)), hydrogen peroxide/formic acid initial concentration ratios (R), and date and time values.

In order to compare with the solar radiation model predictions, UV and total broadband solar radiation fluxes incident on the reactor window were measured by means of CM11 and CUV3 Kipp and Zonen radiometers. Type J thermocouple measurements were used to compare with temperature predictions.

THEORETICAL MODEL

Mass and thermal energy balances

The mass and thermal energy balances for a photoreactor placed inside the loop of a batch recycling system (Figure 1) are given by the following mathematical expressions:

$$\frac{\mathrm{d}}{\mathrm{d}t}\boldsymbol{C}(t) = \frac{V_{\mathrm{irr}}}{V}\langle \boldsymbol{R}(x,t)\rangle_{V_{\mathrm{irr}}} + \frac{V - V_{\mathrm{irr}}}{V}\boldsymbol{R}^{\mathrm{T}}(t) \qquad \boldsymbol{C}(t=0) = \boldsymbol{C}^0 \tag{1}$$

$$\frac{\mathrm{d}}{\mathrm{d}t}T(t) = \eta A_{\mathrm{c}}\, q(t) - \Theta(T - T_{\mathrm{a}}(t)) + Q_{\mathrm{p}} \quad T(t=0) = T^0 \tag{2}$$

where $\boldsymbol{R}$ and $\boldsymbol{R}^{\mathrm{T}}$ are the light-activated (or photo-Fenton) and thermal (or Fenton) reactions, respectively. The first term on the right-hand side of Equation (1) gives the pollutant degradation produced by photo-Fenton reaction occurring in the irradiated liquid volume V_{irr} (the upper channel in the solar reactor). The second term represents the pollutant decomposition generated by the thermal (dark) reaction that takes place in the non-irradiated volume $V - V_{\mathrm{irr}}$. A derivation of the mass balance for a similar recycling system has been reported by Rossetti *et al.* (2002).

Table 2 | Model parameters

Parameter		
Reactor parameters		
Total liquid volume (V)	35	dm^3
Irradiated volume (V_{irr})	6.1	dm^3
Reactor depth (L)	30	mm
Plate thickness (e)	3.2	mm
Optical parameters		
Polycarbonate plate refractive index	1.49	
Water refractive index	1.33	
Air refractive index	1	
Kinetic parameters		
λ-average primary quantum yield ($\bar{\Phi}_{\mathrm{Fe(II)}}$)	0.21*	
Pre-exponential factors†		
$K_{\infty,1}$	1.19×10^{17}	$\mathrm{M}^{-1}\,\mathrm{s}^{-1}$
$K_{\infty,2}$	1.5×10^{9}	$\mathrm{M}^{-1}\,\mathrm{s}^{-1}$
$K_{\infty,3}$	0.14	–
$K_{\infty,4}$	0.07	–
$K_{\infty,5}$	7.77	–
Activation energies†		
E_1	112.86	$\mathrm{kJ\,mol}^{-1}$
E_2	46.76	$\mathrm{kJ\,mol}^{-1}$
Thermal energy balance parameters		
Window area (A_{c})	0.24	m^2
Optical characteristic of reactor (η)	5.35×10^{-6}	$(\mathrm{J\,kg}^{-1}\,°\mathrm{C}^{-1})^{-1}$
Heat losses of device (Θ)	7.99×10^{-5}	$\mathrm{kg\,m}^{-2}\,\mathrm{s}^{-1}$
Ratio of heat input from circulating pump to effective heat capacity of storage tank (Q_{P})	7.89×10^{-4}	$\mathrm{kg\,°C\,s}^{-1}$
Solar radiation parameters		
UV spectral range	[280:450]	nm
Thermal spectral range	[350:2800]	nm
Extraterrestrial spectrum	Gueymard	
Tilt angle	30	(deg)
Surface azimuth counted clockwise from North	0	(deg)

*Bossmann *et al.* (1998).
†The kinetic constant values were obtained from the values reported by Farias *et al.* (2008), within the range of the corresponding 90% confidence interval.

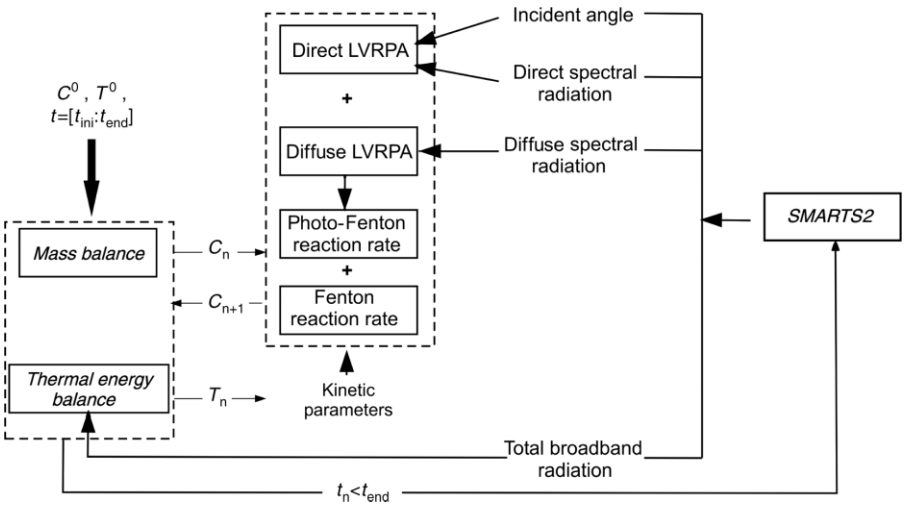

Figure 2 | Calculation procedure.

In Equation (2), T and T_a are the reaction and ambient temperatures, A_c is the window area, q the total broadband solar radiation, Q_p the ratio of heat input from circulating pump to effective heat capacity of storage tank, and η and Θ are parameters relative to the thermal performance of the complete system. These terms represent the optical characteristics of reactor and the heat losses of the device (see Appendix). Q_p, η and Θ were estimated from measurements of the temperature variations of the storage tank from a set of irradiated and non-irradiated experiments without chemical reaction.

Kinetic model

The kinetic modelling of the Fenton and photo-Fenton degradation rates employing formic acid as a model pollutant for relatively low iron concentrations, was proposed by Farias *et al.* (2008). The expressions proposed

Table 3 | RMSE and MAE statistical errors

Experimental Runs	Temperature (°C)	C_P (mM)	C_F (mM)	Total radiation (W m^{-2})	UV radiation (W m^{-2})
RMSE					
1	1.12	0.28	0.11	43.10	1.10
2	1.76	0.21	0.23	10.36	0.78
3	1.24	0.36	0.21	15.82	0.98
4	2.02	0.37	0.21	19.10	0.49
5	0.41	0.07	0.10	–	–
6	1.21	0.60	0.20	57.13	2.52
MAE					
1	0.92	0.23	0.08	21.22	1.06
2	1.46	0.16	0.20	9.77	0.72
3	1.03	0.26	0.17	3.74	0.89
4	1.53	0.29	0.18	15.61	0.41
5	0.35	0.06	0.07	–	–
6	0.76	0.53	0.16	51.10	2.45

Table 4 | Relative errors

	Variables				
	Temperature	C_P	C_F	Total radiation	UV radiation
$NMAE_{variable}(\%)$	4.58	7.79	8.11	4.76	6.32
$NRMSE_{variable}(\%)$	2.91	9.39	10.18	3.66	4.24

to represent the formic acid, hydrogen peroxide, and ferrous ion degradation reactions, are:

$$\begin{bmatrix} R_F(x,t) \\ R_P(x,t) \\ R_{Fe^{2+}}(x,t) \end{bmatrix} = \begin{bmatrix} R_F^T(t) \\ R_P^T(t) \\ R_{Fe^{2+}}^T(t) \end{bmatrix} + \bar{\Phi}_{Fe(II)} \sum_{\lambda} e_{\lambda}^{a}(x,t) \begin{bmatrix} -\frac{1}{\delta} \\ \frac{1}{\delta}\left(1-\frac{\gamma}{\xi}\right) \\ \frac{2}{\delta}\frac{\gamma}{\xi} \end{bmatrix} \quad (3)$$

$$\gamma = K_3 \frac{C_P}{C_F} + 1; \quad \delta = \gamma + K_4 \frac{C_{Fe^{2+}}}{C_F}; \quad \xi = K_5 \frac{C_{Fe^{2+}}}{C_{Fe^{3+}}} + 1 \quad (4)$$

In Equations (3) and (4) $\bar{\Phi}_{Fe(II)}$ is the wavelength averaged primary quantum yield, $e_{\lambda}^{a}(x,t)$ is the Spectral Local Volumetric Rate of Photon Absorption (LVRPA), K_i are kinetic parameters, and C_F, C_P, $C_{Fe^{2+}}$, and $C_{Fe^{3+}}$ are the formic acid, hydrogen peroxide, ferrous ion, and ferric ion concentrations, respectively. The ferric ion concentration as a function of time can be calculated from the initial ferric ion concentration ($C_{Fe^{3+}}^0$) and the actual ferrous ion concentration ($C_{Fe^{2+}}$).

The mathematical expression of the thermal reaction rate (first term on the right hand side of Equation (3)), may be represented by Equation (5).

$$\begin{bmatrix} R_F^T(t) \\ R_P^T(t) \\ R_{Fe^{2+}}^T(t) \end{bmatrix} = -C_P \left\{ \frac{K_2 C_{Fe^{2+}}}{\delta} \begin{bmatrix} 1 \\ \delta - 1 + \frac{\gamma}{\xi} \\ 2\left(\delta - \frac{\gamma}{\xi}\right) \end{bmatrix} + \frac{K_1 C_{Fe^{3+}}}{\xi} \begin{bmatrix} 0 \\ 1 \\ -2 \end{bmatrix} \right\} \quad (5)$$

An experimental design based on the D-optimality criterion was adopted to avoid simultaneous high reaction temperatures and iron concentrations and, consequently, the precipitation of iron compounds. By applying a non-linear regression procedure, the Arrhenius kinetic parameters between 20 to 55°C were estimated.

Radiation field

In a previous work, Rossetti *et al.* (1998) proposed and experimentally verified a rigorous radiation field model for a flat-plate solar photoreactor. The authors assumed that only radiation absorption took place in the reacting medium and that the glass window was irradiated with direct and diffuse solar radiation. In the present work, an analogous expression is proposed to predict the monochromatic LVRPA as a function of position × inside the solar photoreactor. The direct or beam (B) and diffuse (D) solar radiation components have been taken into account in the expressions for calculating the LVRPA:

$$e_{\lambda}^{a}(x,t) = e_{B,\lambda}^{a}(x,t) + e_{D,\lambda}^{a}(x,t) \quad (6)$$

$$e_{B,\lambda}^{a}(x,t) = \kappa_{\lambda}(t)\, q_{B,\lambda}(t)\, T_{B,\lambda}(\mu_i) \exp\left[-\kappa_{T,\lambda}(t)\, x/\mu_{ref}\right] \quad (7)$$

$$e_{D,\lambda}^{a}(x,t) = 2\kappa_{\lambda}(t)\, q_{D,\lambda}(t)\, T_{D,\lambda}\, E[x, \kappa_{\lambda}(t)] \quad (8)$$

Here $q_{B\lambda}$ and $q_{D\lambda}$ are the direct and diffuse solar radiation for a give wavelength, $T_{B\lambda}$ and $T_{D\lambda}$ are the direct and diffuse transmittances, κ_{λ} is the spectral volumetric absorption coefficient of the absorbing species, μ_{ref} and μ_i are the cosines of refraction and incident angles, and E is the second order exponential integral function. In Equations (7) and (8) we have also defined:

$$T_{B,\lambda}(\mu_i) = \frac{T_{1,\lambda}(\mu_i) T_{2,\lambda}\left(\mu_i'\right)}{1 - R_{1,\lambda}(\mu_i) R_{2,\lambda}(\mu_i')} \qquad T_D = T_B[\mu_i = \cos(60°)] \quad (9)$$

$$T_{i,\lambda} = \frac{\tau_{\lambda}(\mu_{ref})(1-\rho_{nm})(1-\rho_{uv})}{\left[1 - \tau_{\lambda}^2(\mu_{ref})\rho_{uv}\rho_{nm}\right]}$$
$$R_{i,\lambda} = \rho_{nm} + \frac{\tau_{\lambda}^2(\mu_{ref})(1-\rho_{nm})\rho_{uv}}{\left[1 - \tau_{\lambda}^2(\mu_{ref})\rho_{uv}\rho_{nm}\right]} \quad (10)$$

$$\tau_{\lambda}(\mu_{ref}) = \exp\left[-\kappa_{\lambda}(t)\frac{e}{\mu_{ref}}\right] \quad (11)$$

where $T_{i,\lambda}$ and $R_{i,\lambda}$ ($i = 1, 2$) are the direct transmittance and reflectance for each plate. In Equation (10) ρ_{nm} and ρ_{uv} are the interface reflectivities, and e the plate thickness.

Numerical solution

The proposed model takes into account the variations of solar radiation with time (or with the zenith angle).

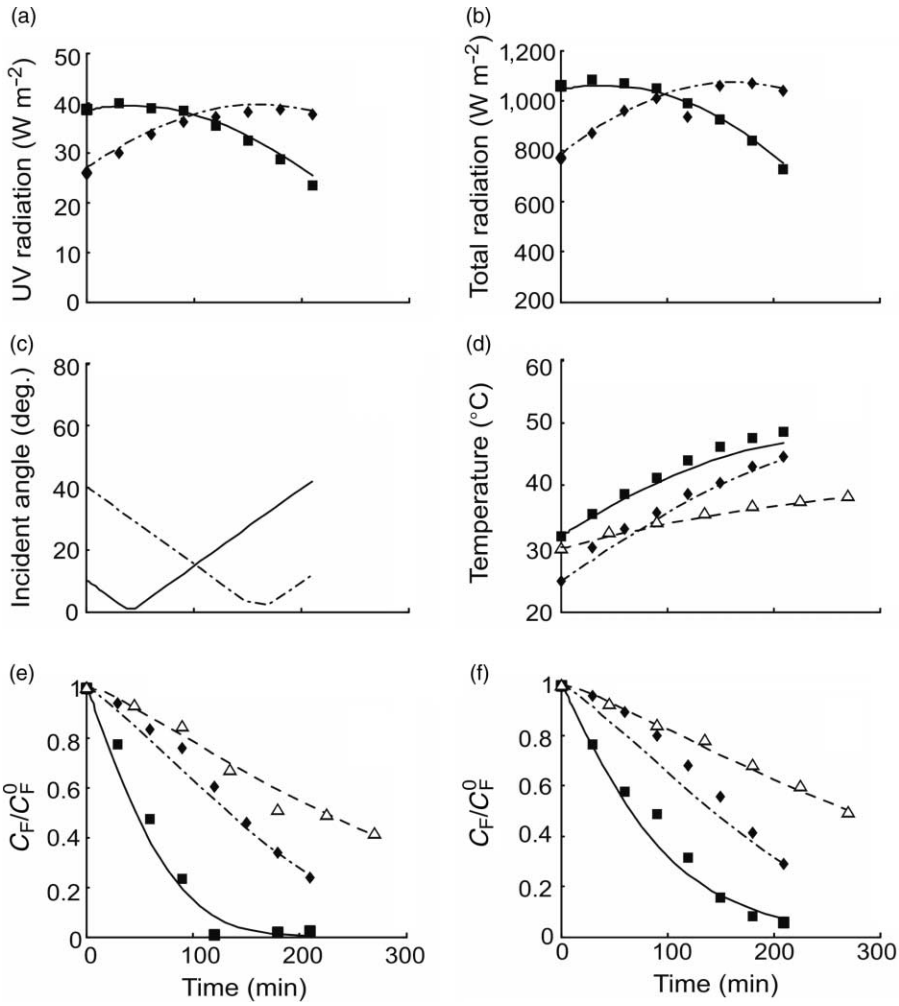

Figure 3 | Model predictions (lines) and experimental data (symbols) vs. time for $C_F^0 = 3$ mM. Keys for non-irradiated reaction: run 5 (- - -, △). Keys for irradiated reaction: run 1 (– · –, ◆), run 3 (—, ■).

To do this, the SMARTS2 program (Gueymard 1995) was called in every loop of the numerical algorithm for solving the ordinary differential equation system (Equations (1) and (2)). Table 2 presents a summary of the main model parameters and Figure 2 gives a representation of calculation procedure.

The SMARTS2 predictions were obtained for Santa Fe (31°39′S, 60°43′W, 8 m above sea level), Argentina. The characteristic values of the Rural–Urban aerosol parameters in the UV and total radiation ranges were obtained from Piacentini *et al.* (2002) and Gueymard *et al.* (2002), respectively. These values were updated for each time of the calculation, in the same form that the surface pressure, ground level air temperature and ground-level relative humidity (%). Finally, the data of ozone total column were taken from the measurements of the TOMS/NASA instrument.

RESULTS: EXPERIMENTAL VALIDATION

Comparison between predicted and experimental results

A root mean square error (RMSE) and a mean absolute error (MAE) have been used to evaluate the accuracy of the model. Results are summarized in Table 3.

Table 4 shows relative errors for the predicted variables. The normalized mean absolute error (NMAE) represents

the error weight in predicted values. The percent mean error of model predictions for all investigated variables was lower than 11%. The normalized root mean square errors (NRMSE) of the model predictions were 2.91, 9.39, 10.18, 3.66, and 4.24% for temperature, hydrogen peroxide and formic acid concentrations, and total and UV broadband solar radiation, respectively.

Results for typical experimental runs

Figure 3 represents model predictions and experimental data as a function of time for irradiated and non-irradiated experiments. The following results are depicted in this figure: (a) UV solar radiation, (b) total solar radiation, (c) incident angle of direct radiation on reactor window, (d) reaction temperature, (e) formic acid relative concentration, and (f) hydrogen peroxide relative concentration.

Notice that the non-irradiated reaction rate is always lower than irradiated reaction rate; even for the highest Fe(III) and R values. The combinated effect of UV/Visible and thermal sunlight is able to degrade at least 70% of formic acid initial concentration after 210 min for relatively low iron concentrations. Moreover, for a ferric ion concentration of 3.5 ppm, the organic pollutant conversion is 98%.

In order to asses the effect of the solar radiation on the reactor performance, experimental runs 3 (irradiated reaction) and 5 (non-irradiated reaction) were performed. These experiments were carried out with similar formic acid initial concentrations and hydrogen peroxide/formic acid initial concentration ratios. Note that, after 180 min of operation, the pollutant conversion with the irradiated reactor was 98.4% versus 49.4% for the dark reactor.

Thus, for all the operating conditions employed in this work, it was possible to predict the performance of a solar reactor for the degradation of a model compound, as a function of the reaction time.

CONCLUSIONS

A novel photoreactor has been presented. It is a hybrid solar unit that captures the thermal and photochemical solar radiation to promote the photo-Fenton degradation of a model compound.

A reactor model was proposed and experimentally verified, using formic acid as a model pollutant. It was possible to predict the solar reactor performance as a function of the reaction time, for different operating conditions. To do this, variations of the spectral UV and total broadband solar irradiances were taken into account by the proposed model.

A good agreement for formic acid and hydrogen peroxide concentrations, reaction temperature, and total and UV broadband solar radiations was obtained. The normalized root mean square errors (NRMSE) of the model predictions for the investigated variables were lower than 11%.

ACKNOWLEDGEMENTS

The authors are grateful to Universidad Nacional del Litoral (UNL), Consejo Nacional de Investigaciones Científicas y Técnicas (CONICET) and Agencia Nacional de Promoción Científica y Tecnológica (ANPCyT). They also thank Antonio C. Negro for his valuable help during the experimental work.

REFERENCES

Alfano, O., Bahnemann, D., Cassano, A., Dillert, R. & Goslich, R. 2000 Photocatalysis in water environments using artificial and solar light. *Catal. Today* **58**(2), 199–230.

Allen, A., Hochanadel, C., Ghormley, J. & Davis, J. 1952 Decomposition of water and aqueous solutions under mixed fast neutron and gamma radiation. *J. Phys. Chem.* **56**, 587–594.

APHA, AWWA, WEF 1995 *Standard Methods for the Examination of Water and Wastewater*, 19th edition. APHA, Washington, pp. 3–68.

Bossmann, S., Oliveros, E., Göb, S., Siegwart, S., Dahlen, E., Payawan, L., Straub, M, Jr., Wörner, M. & Braun, A. 1998 New evidence against hydroxyl radicals as reactive intermediates in the thermal and photochemically enhanced Fenton reactions. *J. Phys. Chem. A* **102**, 5542–5550.

Farias, J., Albizzati, E. & Alfano, O. 2007 Solar degradation of formic acid: temperature effects on photo-Fenton reaction. *Ind. Eng. Chem. Res.* **46**(23), 7580–7586.

Farias, J., Albizzati, E. & Alfano, O. 2008 Kinetic study of the photo-Fenton degradation of formic acid. Effects of temperature and iron concentration. *Catal. Today* **144**, 117–123.

Gernjak, W., Fuerhacker, M., Fernández-Ibañez, P., Blanco, J. & Malato, S. 2006 Solar photo-Fenton treatment-process parameters and process control. *Appl. Catal. B Environ.* **64**(1–2), 121–130.

Gueymard, C. 1995 *SMARTS2, a simple model of the atmospheric transfer of sunshine: algorithms and performance assessment*. Report FSEC-PF-270-95, Florida Solar Energy Center, Florida.

Gueymard, C., Myers, D. & Emery, K. 2002 Proposed reference irradiance spectral for solar energy systems testing. *Solar Energy* **73**(6), 443–467.

Malato, S., Fernández-Ibáñez, P., Maldonado, M., Blanco, J. & Gernjak, W. 2009 Decontamination and disinfection of water by solar photocatalysis: recent overview and trends. *Catal. Today* **147**, 1–59.

Monteagudo, J., Durán, A., San Martín, I. & Aguirre, M. 2009 Effect of continuous addition of H_2O_2 and air injection on ferrioxalate-assisted solar photo-Fenton degradation of Orange II. *Appl. Catal. B Environ.* **89**, 510–518.

Piacentini, R., Alfano, O., Albizzati, E., Luccini, E. & Herman, J. 2002 Solar ultraviolet irradiance for clear sky days incident at Rosario, Argentina: measurements and model calculations. *J. Geophys. Res. D Atmos.* **107**(15), 6-1–6-7.

Rossetti, G., Albizzati, E. & Alfano, O. 1998 Modeling and experimental verification of a flat-plate solar photoreactor. *Ind. Eng. Chem. Res.* **37**(9), 3592–3601.

Rossetti, G. H., Albizzati, E. D. & Alfano, O. M. 2002 Decomposition of formic acid in a water solution employing the photo-Fenton reaction. *Ind. Eng. Chem. Res.* **41**, 1436.

Sagawe, G., Lehnard, A., Lübber, M. & Bahnemann, D. 2001 The insulated solar fenton hybrid process: fundamental investigations. *Helvetica Chim. Acta* **84**(12), 3742–3759.

Zapata, A., Oller, I., Bizani, E., Sánchez-Pérez, J., Maldonado, M. & Malato, S. 2009 Evaluation of operational parameters involved in solar photo-Fenton degradation of a commercial pesticide mixture. *Catal. Today* **144**, 94–99.

APPENDIX

Thermal energy balance

Starting from a thermal energy balance in a well mixed, batch recycling reactor, one can write:

$$C_T \frac{\mathrm{d}T}{\mathrm{d}t} = \eta_o A_c q_T(t) - (\mathrm{UA})_R (T - T_a(t)) - (\mathrm{UA})_{Tk} (T - T_a(t)) + Q_P' \quad (A.1)$$

In this equation, the solar radiation absorbed per unit area of reactor window is represented by the product of the optical efficiency η_o times the total broadband incident radiation flux q_T. The second term of Equation (A.1) is the thermal energy loss from the reactor to the surroundings, computed as the product of the reactor heat loss coefficient $(\mathrm{UA})_R$ times the difference between the temperature of the system and the ambient temperature $(T - T_a)$. The third term represents the thermal energy loss from the storage tank to the surroundings, calculated as the product of the tank heat loss coefficient $(\mathrm{UA})_{Tk}$ and the temperature difference $(T - T_a)$. Finally, the fourth term is the constant heat input from the circulation pump (Q_P').

We can define the following thermal energy parameters:

$$\eta = \frac{\eta_o}{C_T} \qquad \Theta = \frac{(\mathrm{UA})_{Tk} + (\mathrm{UA})_R}{C_T} \qquad Q_P = \frac{Q_P'}{C_T} \quad (A.2)$$

Substituting Equation (A.2) into Equation (A.1), we finally obtain Equation (2) of the main body of the paper:

$$\frac{\mathrm{d}}{\mathrm{d}t} T(t) = \eta A_c\, q(t) - \Theta (T - T_a(t)) + Q_p \qquad T(t = 0) = T^0 \quad (A.3)$$